Polarization Effects in High-Speed Train Radio Communications Channels

S. Knörzer[1] ***and W. Wiesbeck***[2]

Institut für Höchstfrequenztechnik und Elektronik, Universität Karlsruhe (TH),
Kaiserstraße 12, 76131 Karlsruhe, Germany
Phone: +49 721 608 2525, Fax: +49 721 691865
E-Mail: [1] Sandra.Knoerzer@ihe.uka.de, [2] Werner.Wiesbeck@ihe.uka.de

Abstract

This paper characterizes the polarization dependence of the high-speed train communications channel. With a three-dimensional ray tracing simulation tool the narrow-band channel characteristics are determined for various polarizations and two typical environments. The results show that the channel characteristics can be optimized by selecting the proper polarization. For this purpose two options result: either the long-term fading amplitude can be maximized or the short-term fading can be minimized.

1. Introduction

For wireless train communications systems the Global System for Mobile Communications-Rail (GSM-R) or the Universal Mobile Telecommunications System (UMTS) are standards for passenger communications. Both provide only very limited data rates. For future rail communications systems an Orthogonal Frequency Division Multiplexing (OFDM) [1] based approach promises higher data rates [2]. With the expected higher data rates not only passenger, but also train control systems could be operated. The high-speed train communications channel has been published in [3] emphasizing the aspect of omnidirectional versus directional antennas. This paper highlights the effect of polarization in this specific environment. Current communications antennas are mounted on the train's roof, based on the principle of $\lambda/4$-antennas, which requires an adequate metallic ground plane (with λ being the wavelength). This $\lambda/4$-monopole antenna features vertical polarization. Apart from GPS (Global Positioning System) all train communications systems operate with vertical polarization. This includes especially GSM-R and UMTS. In non-railway environment mobile communications systems, X-polarized antennas are usually installed in order to consider the arbitrary alignment of the mobiles and to exploit the channel diversity. In contrast to handheld mobile devices the alignment of the train antenna will not change with the train motion in polarization, in elevation and merely little in azimuth. Characteristic for high-speed train tracks is the widely stretched environment along the track with predictable objects (e.g. pylons) at both sides. The question arises if a preferential polarization exists for the specific environment of high-speed train tracks, which could outperform the widespread vertical polarization.

In Sect. 2 the wave propagation model for the simulations is introduced. The description of the implemented typical scenarios for high-speed train tracks and the various test polarizations are presented in Sect. 3. This is followed by the presentation of the simulation results with respect to the long-term and short-term fading in Sect. 4. The paper closes with a summary of the main findings in the conclusion.

2. Wave Propagation Model Including Dipole Antenna Characteristics

At the Institut für Höchstfrequenztechnik und Elektronik a three-dimensional ray tracing algorithm has been developed and implemented ([4], [5]). This simulation tool takes different propagation effects and their combinations into account: multiple reflections, multiple diffractions and scattering. Furthermore, a three-dimensional antenna characteristic is assigned to the transmitter and the receiver. In this paper a $\lambda/2$-dipole characteristic is implemented for all antennas and tilted to obtain the corresponding polarizations with the transmitter and the receiver antenna being co-polarized. The antenna characteristic is chosen according to real communications systems where $\lambda/2$-dipoles and their derivatives are often used for mobile stations (MSs) and base stations (BSs) (usually several in an array). All simulations are carried out at a frequency of 5.2 GHz where IEEE 802.11a operates.

3. Scenarios, Coordinate System and Polarizations

The simulations are performed in two typical high-speed train scenarios. One scenario is called noise barrier scenario and the other vegetation scenario. As implied by the names in the first scenario noise barriers are on both sides of the track and in the latter vegetation i.e. trees. The noise barrier is modeled as a concrete wall, which allows reflection and diffraction. To the trees a diffuse scattering wave propagation characteristic is assigned. Further objects are present in both scenarios: a concrete ground, two pairs of tracks and a pair of pylons every 65 m along the track (in y-direction). The overall y-length of each simulated scenario is 2000 m. Fig. 1 shows a schematic xz-plane cross-section of the noise barrier scenario.

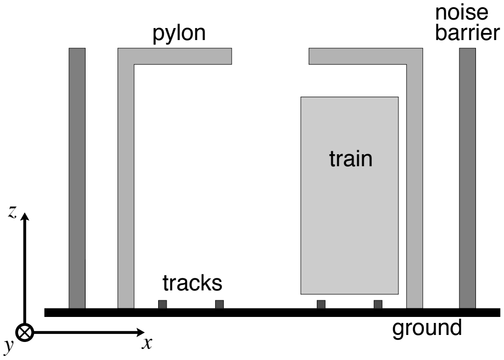

Figure 1: xz-plane cross-section of the noise barrier scenario (not true to scale)

The high-speed train is modeled according to the dimensions of the German InterCity Express (205 m long, 3 m wide, 3.8 m high) and perfect conducting metal is assigned as material. On the roof approximately in the middle of the train (100 m from the rear end) the mobile antenna characteristic is attached. The train including the antenna moves in positive y-direction. This movement is implemented in the simulation by placing the train at sequential positions in the scenario (called snapshots) and assigning the corresponding velocity (111.1 m/s) to the train. The simulation results from the series of snapshots represent the time-variance of the channel. The transmitter consists of several BSs working in the common frequency mode. The transmit antennas are placed marginally higher than the train antenna beside the train track at a y-position every 500 m in the scenario. For the simulation the three nearest BSs to the mobile antenna are active, i.e. $y_{\mathrm{BS1}} = 500\,\mathrm{m}$, $y_{\mathrm{BS2}} = 1000\,\mathrm{m}$, $y_{\mathrm{BS3}} = 1500\,\mathrm{m}$. This results in a simulation range of 500 m around BS2. At train antenna positions smaller than $y = 750\,\mathrm{m}$ or larger than $y = 1250\,\mathrm{m}$ another base station trio would be switched on and the results from the 500 m range would recur. With a simulation range of 500 m and the given velocity of 111.1 m/s the total simulated time period is 4.5 s.

In the following characteristic channel quantities of various polarizations are compared and assessed. Four polarizations are considered. For the vertical polarization the electric field vector of the $\lambda/2$-dipole is aligned with the z-axis. The horizontal $\perp$ and horizontal $\|$ polarization are parallel to the x-axis and y-axis, respectively. In the last case, the $45°$ polarization, the electric field vector is tilted by $45°$ in y-axis direction with reference to the vertical polarization. The BS antenna and MS antenna are in all simulations co-polarized with a transmit power of 1 W.

4. Long-Term and Short-Term Fading Results

In this section the long-term and short-term fading results are presented for the scenarios and polarizations described in the previous sections. In each figure four curves are given corresponding to the four polarizations. The vertical polarization is considered as the reference case in the following. The long-term fading is extracted from the complex transmission factor of a channel impulse response by applying a windowing over 80λ. This value is proposed in literature (cf. [6]) and reasonable for the considered radio channels. The short-term fading is subsequently calculated by dividing the transmission factor by the long-term fading. Both, the long-term and the short-term fading reveal precious radio channel information for system designers. On the one hand, the long-term fading offers the possibility to compare the amplitude in quantity. Higher amplitudes which usually mean higher signal-to-noise ratios allow wider ranges for a communications system (e.g. further BS distances or lower bit error rates assuming a constant data rate). Up to a certain amount, the variations in the long-term fading amplitude can be compensated by an automatic gain control (AGC). On the other hand, the short-term fading characterizes the fast signal drops which cause system outages as soon as the signal falls below a system dependent threshold. Finally, this results in data loss. The abrupt signal drops of the short-term fading can not be outweighed by an AGC as it's reaction time is too long. The short-term fading can be characterized by the cumulative distribution function (CDF) which provides the probability that the signal is equal or less than a certain value. A steeper ascent of the CDF means less pronounced variations of the short-term fading. In general, the wider the CDF moves to the right for low probabilities (cf. Figs. 4 and 5; a detailed description of these figures follows two paragraphs later) the easier for a communications system and the less outages.

In Figs. 2 and 3 the long-term fading is plotted for the noise barrier and vegetation scenario for all considered polarizations. As there exists a strong line-of-sight path from BS2 to the train antenna, the long-term fading amplitude increases and decreases with the mobile train antenna approaching BS2 and departing again. This can be seen for all polarizations. The moment of passing BS2 is related to the time instant $t = 2.25\,\mathrm{s}$. Apparently, the signal amplitude of the horizontal $\parallel$ polarization is for most times lower than for all other polarizations. This results from the antenna alignment where the $\lambda/2$-dipoles of the BSs and MS are all parallel to the y-axis. This means the line-of-sight paths between the BSs and MS depart and arrive at the antennas close to the nulls of the antenna characteristics. Only while passing BS2 the signal amplitude increases to a level comparable to the other polarizations because the strong line-of-sight path from BS2 to MS passes the antenna characteristic in its main beam. As a result of the long-term fading the application of horizontal $\parallel$ polarization is not feasible. An attenuation of the signal compared to the vertical polarization can furthermore be observed for the 45° polarization. The approximately 8 dB difference at train antenna positions far from BS2 is an effect completely due to the antenna characteristic as well. In case of an isotropic antenna the curves for vertical and 45° polarization would tally. Most of the propagation paths depart and arrive within the $\theta = 90^\circ$ plane as the BS and MS antennas are situated at approximately the same height. In this propagation plane solely the antenna characteristic for the vertical polarization corresponds constantly to the main beam of the $\lambda/2$-dipole (omnidirectional in the propagation plane). Hence, the vertical polarization shows the highest signal amplitude during most time instants. Even the horizontal $\perp$ polarization which partly surmounts the vertical polarization shows attenuation effects due to the antenna characteristic null at the moment of passing BS2. All remaining deviation effects of the long-term fading amplitudes can be deduced from the different reflection and diffraction coefficients of the different polarizations. Considering the long-term fading the vertical and horizontal $\perp$ polarization yield the best performance.

The short-term fading is presented in Figs. 4 and 5. The influence of a non-omnidirectional antenna pattern in the propagation plane disappears for the short-term fading in contrast to the long-term fading. Hence, the different curves, except the curve for horizontal $\parallel$ polarization where the heavy attenuation inhibits reasonable values, represent merely the polarization impact. In the noise barrier scenario the horizontal $\perp$ polarization clearly outperforms the other polarizations. At a cumulative probability of 0.1 (10% value) the amplitude of the short-term fading is -4.2 dB for the horizontal $\perp$ polarization. Compared to the remaining polarizations with a 10% value of -6.2 dB this is an enhancement of 2.0 dB. However, the situation is different for the vegetation scenario. In this case the vertical and 45° polarizations show the least deep short-term signal drops. Except for the horizontal $\parallel$ curve all curves show a

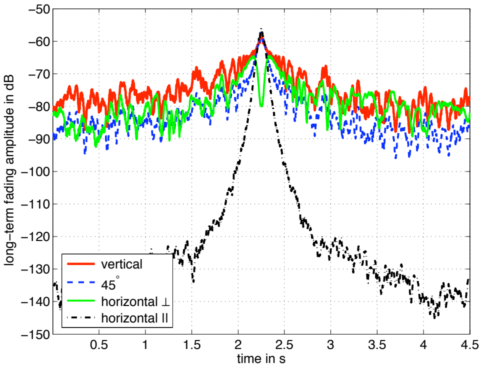

Figure 2: Long-term fading, noise barrier scenario

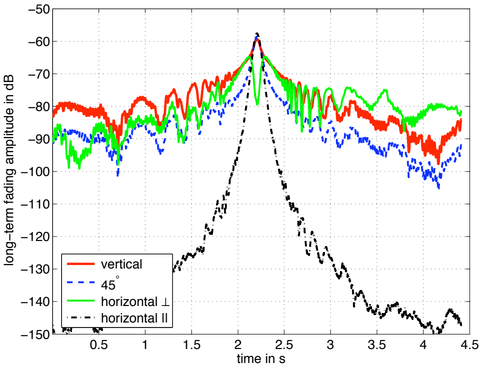

Figure 3: Long-term fading, vegetation scenario

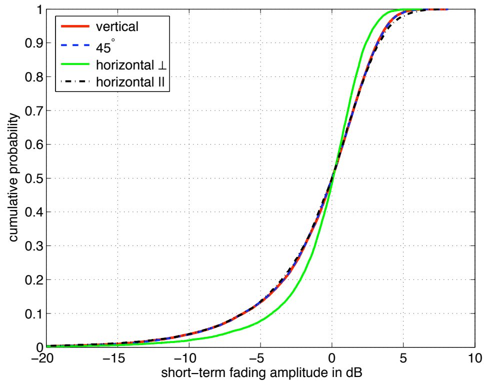

Figure 4: CDF, noise barrier scenario

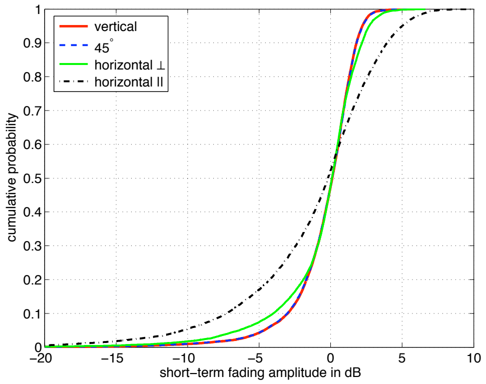

Figure 5: CDF, vegetation scenario

steeper slope for the vegetation scenario which means that this is not the limiting environment. The 10% values for the vertical and 45° polarizations increase by 3.2 dB to a value of -3.0 dB while the value for the horizontal || curve degrades to -7.3 dB. The horizontal ⊥ curve changes only very little to a 10% value of -4.0 dB. This is an advantage for horizontal ⊥ polarization as the short-term channel characteristics are more or less independent of the scenario.

5. Conclusion

The channel model introduced in this paper is based on three-dimensional ray-optical wave propagation modeling in two realistic high-speed train scenarios. Characteristic quantities of the radio channel are calculated from simulations using $\lambda/2$-dipole antennas and four different polarizations. The results are assessed with reference to the vertical polarization that is currently used in train communications systems. The vertical polarization shows the highest long-term fading amplitude. The horizontal || polarization presents a considerably lower long-term fading amplitude which disqualifies it from the use in a communications system. Considering the CDF the horizontal ⊥ polarization trumps the vertical polarization while the long-term fading amplitude is moderately lower compared to vertical polarization. Apart from the CDF evaluation the vertical polarization outperforms the considered alternative polarizations. Thus, in the specific environment of high-speed trains it is generally recommended to stick to vertically polarized antennas for communications purposes. However, if the intended communications system is very susceptible for rapid signal drops a horizontal ⊥ polarization should be preferred.

6. References

[1] S. Weinstein and P. Ebert, “Data Transmission by Frequency-Division Multiplexing Using the Discrete Fourier Transform,” *IEEE Transactions on Communication Technology*, vol. 19, no. 5, pp. 628–634, 1971.

[2] M. Russell and G. Stuber, “Interchannel Interference Analysis of OFDM in a Mobile Environment,” *Proceedings of the 42nd IEEE Vehicular Technology Conference*, vol. 2, pp. 820–824, July 1995.

[3] S. Knörzer, M. A. Baldauf, T. Fügen, and W. Wiesbeck, “Channel Analysis for an OFDM-MISO Train Communications System Using Different Antennas,” *Proceedings of the 66th IEEE Vehicular Technology Conference*, vol. CD-ROM, October 2007.

[4] J. Maurer, T. Fügen, S. Knörzer, and W. Wiesbeck, “A Ray-Optical Approach to Model the Inter-Vehicle Transmission Channel,” *Frequenz, Journal of RF-Engineering and Telecommunications*, vol. 60, pp. 95–98, May/June 2006.

[5] T. Fügen, J. Maurer, T. Kayser, and W. Wiesbeck, “Capability of 3-D Ray Tracing for Defining Parameter Sets for the Specification of Future Mobile Communications Systems,” *IEEE Transactions on Antennas and Propagation*, vol. 54, pp. 3125–3137, November 2006.

[6] W. Lee, *Mobile Communications Engineering*. McGraw-Hill, 1982.